Journal of Earthquake Engineering

ISSN: (Print) (Online) Journal homepage: https://www.tandfonline.com/loi/ueqe20

A Generalized Artificial Neural Network for Displacement-Based Seismic Design of Mass Timber Rocking Walls

Da Huang & Shiling Pei

To cite this article: Da Huang & Shiling Pei (2021): A Generalized Artificial Neural Network for Displacement-Based Seismic Design of Mass Timber Rocking Walls, Journal of Earthquake Engineering, DOI: 10.1080/13632469.2021.1988768

To link to this article: https://doi.org/10.1080/13632469.2021.1988768

Published online: 26 Oct 2021.

JOURNAL OF EARTHQUAKE ENGINEERING
https://doi.org/10.1080/13632469.2021.1988768

Taylor & Francis
Taylor & Francis Group

A Generalized Artificial Neural Network for Displacement-Based Seismic Design of Mass Timber Rocking Walls

Da Huang and Shiling Pei

Department of Civil & Environment Engineering, Colorado School of Mines, Golden, Colorado, USA

ABSTRACT

Displacement-based seismic design often requires nonlinear time history simulation of building responses which is computationally intensive. This technical note presents an artificial neural network (ANN) designed to generate max inter-story drift for buildings with post-tensioned mass timber (MT) rocking walls systems. This particular lateral system was selected because it is an innovative system with limited physical design parameters, making it an ideal candidate for ANN. The proposed model achieved significantly higher computational efficiency than time history simulation, while maintaining similar level of accuracy. The proposed method could potentially be used for automated design of MT rocking wall lateral systems.

ARTICLE HISTORY
Received 7 May 2021
Accepted 3 August 2021

KEYWORDS
Artificial neural network; max dynamic response prediction; displacement-based seismic design; mass timber building; CLT post-tensioned rocking wall

1. Introduction

Mass timber building has emerged in recent years as a viable option for multi-story urban infill archetype. With the advantage of lightweight and relatively lean on-site construction processes, mass timber lateral systems are gaining traction among researchers for regions with high seismicity. One new structural system that is believed to be able to provide performance and economy is post-tensioned cross-laminated timber (CLT) rocking wall system. Similar to post-tensioned concrete rocking wall system (Nazari, Sritharan, and Aaleti 2017), mass timber rocking wall mainly consists of a monolithic mass timber panel with vertical post-tensioning (PT) elements anchored to the foundation to provide self-centering ability. Supplemental energy dissipation devices (e.g., friction damper, U-shaped flexural plate (UFP)) can also be added to the wall panel to provide additional damping. Post-tensioned mass timber walls were studied by a handful of researchers in New Zealand and North American (Akbas et al. 2017; Buchanan et al. 2008; Perez, Sause, and Pessiki 2007; Priestly 1991). Particularly, a series of static and dynamic tests of CLT rocking walls conducted in recent years (Chen, Popovski, and Iqbal 2020; Ganey et al. 2017; Moroder et al. 2018; Pei et al. 2019) demonstrated the advantage and practicality of adopting such a lateral system for resilient multi-story wood buildings. Mass timber rocking wall system has been used in real building projects in New Zealand (Buchanan et al. 2008) and permitted in the U.S. (framework (Haselton et al. 2017a, 2017b; Jarrett et al. 2017; Zimmerman et al. 2017)).

Because mass timber rocking wall system has not been recognized by existing design codes (e.g., ASCE 2017, IBC 2018), an alternative performance-based seismic design (PBSD) approach must be employed in practice. One of the most popular PBSD approaches for building design is the displacement-based design, which focuses on controlling maximum inter-story drift. During this process, the designer must be able to confidently predict building dynamic response using a numerical model. Recently, serval numerical models were developed and validated (Massari, Savoia, and Barbosa 2017; Pei et al. 2021) for mass timber rocking wall systems using shake table test data. While these models

CONTACT Da Huang huang@mines.edu Department of Civil & Environment Engineering, Colorado School of Mines, 1500 Illinois St, Golden, CO 80401.

can simulate the max dynamic response with reasonable accuracy, they are very complicated and computationally expensive for trial-and-error style displacement-based design. The main objective of this study is to develop a generalized ANN model that can predict max inter-story drift of mass timber rocking wall system with significantly higher efficiency than traditional time history integration models.

ANN models have been widely recognized as powerful machine learning tools in civil engineering. Specifically, for dynamic response prediction, two types of machine learning tools were explored in the existing literature. The first type focuses on a specific structure under a limited number of earthquake ground motions (Jeng and Mo 2004; Nguyen et al. 2020; Sahoo and Chakraverty 2018; Wang et al. 2009). These models used different machine learning methods such as ANN, Recurrent neural network (RNN), Convolutional neural network (CNN), Long short-term memory network (LSTM network) in order to achieve the best prediction outcome. For example, Nguyen et al. (2020) developed an optimized ANN for dynamic response prediction for short buildings under Chi-Chi 1999 earthquake, Jeng and Mo (2004) used multilayer perception (MLP) networks with backpropagation algorithm for quick response estimations for prestressed concrete bridge under 1940 EI Centro earthquake. Sahoo and Chakraverty (2018) proposed an application of functional link neural networks (FLNNs) for structural response prediction of tall buildings due to seismic loads. Wang et al. (2009) used the first 4 s of the dynamic response of a bridge structure as training data for ANN to predict responses in the next 4 s under one earthquake. After training, these models can achieve good accuracy but were not generalized. The second type is more generalized as they were trained for prediction under different earthquakes, but they are mostly still structure-specific (Abd-Elhamed, Shaban, and Mahmoud 2018; Lagaros and Papadrakakis 2012; Perez-Ramirez et al. 2019; Zhang et al. 2019; Zhang, Liu, and Sun 2020). For example, Lagaros and Papadrakakis (2012) conducted an ANN network scheme for nonlinear seismic response of 2-story reinforced concrete 3D buildings, Zhang et al. (2019), Zhang, Liu, and Sun (2020) developed a deep LSTM network for nonlinear structural response prediction, and further refined the model by taking the laws of physic as extra constraints. Abd-Elhamed, Shaban, and Mahmoud (2018) used the Logical analysis of data (LAD) method for SDOF building and compared the performance of LAD and ANN. Perez-Ramirez et al. (2019) utilized the Non-linear autoregressive exogenous (NARX) network with Bayesian regularization for response prediction of a 1:20 scaled 38-story residential building. In addition, some of these machine learning approaches are computationally expensive.

In this study, A generalized ANN architecture is proposed for max response prediction for mass timber rocking wall systems. This model is formulated to be highly efficient computationally while using physical design parameters of the rocking wall system as input in order to facilitate the trail-and-error style design process. The ANN was trained using simulated data generated from a test-validated numerical model within a representative parameter space for realistic design conditions. The model is intended to serve as a useful tool for initial design iterations in performance-based seismic design of mass timber rocking wall systems where extremely fast estimation of max seismic response is necessary.

2. Methodology

The objective of the proposed ANN is to enable fast prediction of inter-story drift response of a multi-story building with a mass timber rocking wall system as shown in Fig. 1. Cross-laminated timber (CLT) is a very popular panel product used in mass timber construction and can be used to form rocking wall lateral systems. CLT rocking wall systems usually contain panelized CLT walls, vertical post-tensioned elements anchored to the foundation, energy dissipation devices (e.g. U-shaped steel plate (UFP), Resilient Slip Friction (RSF) joint). These supplemental damping devices typically are attached to the boundary column and reduce drift demands while the system rocks at the edge of the CLT rocking wall panel. Rocking wall system is typically balloon-framed into the building and carries

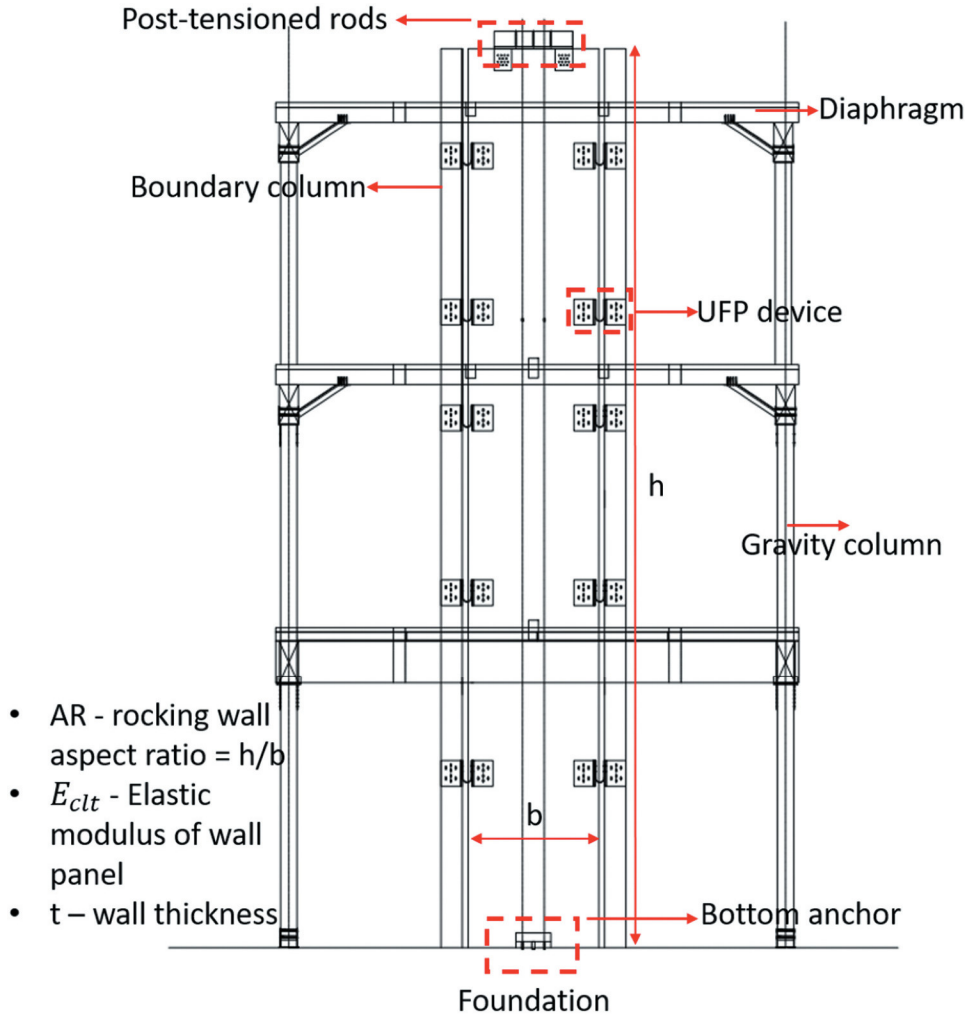

Figure 1. CLT rocking wall conceptual configuration.

only lateral loads. A slotted shear key connection is responsible to transfer lateral load from diaphragms to the wall without engaging the wall under gravity loads. A realistic example of a post-tensioned CLT rocking wall can be found in Pei et al. (2019).

The objective of this study is to develop an ANN model for maximum displacement prediction for mass timber rocking walls. The structure of an ANN model can be defined by its input and output parameters, as well as the internal layered neural structure. Since this study was focused on maximum drift response prediction, the output of the ANN is a single parameter, namely maximum inter-story drift of the building during an earthquake. The input parameters contain two main categories, namely the earthquake ground motion parameters, and rocking wall design parameters (see Fig. 1). The structure of the ANN input/output parameters is listed in Table 1.

Note that some of the wall design input parameters are physical parameters such as wall height (i.e., building height) and aspect ratio, while other parameters are derived parameters from a physical system, such as $K0_{ufp}$K0$_{\mathrm{ufp}}$ for energy dissipation devices (Baird et al. 2014). In a practical design setting, those derived parameters can easily be calculated using the physical design parameters of these devices, which will dictate the supplement damping of the design explicitly. In addition to the UFP device contribution, the damping ratio used to generate the training dataset is randomly selected by

Table 1. ANN input/output parameters.

		Wall design input			
EQ input		Basic geometry	Wood	PT	UFP
Sa@0.1s	Spectrum acceleration at 0.1s	N_{st} – story number	E_{clt} – elastic modulus of CLT	F_{ini}/F_y – ratio of PT initial force and yield force	$K0_{ufp}$ – total initial stiffness of UFP
Sa@0.5s	Spectrum acceleration at 0.5s	m_1 – story mass	AR – aspect ratio of wall		
Sa@1s	Spectrum acceleration at 1s				
Sa@2s	Spectrum acceleration at 2s	h_1 – story height		A_{pt} – total area of PT	dy_{ufp} – yielding deformation of UFP
Sa@3s	Spectrum acceleration at 3s		t – thickness of wall		
Sa@Tn	Spectrum acceleration at Tn	ζ – damping ratio			
PGA	Peak ground acceleration				

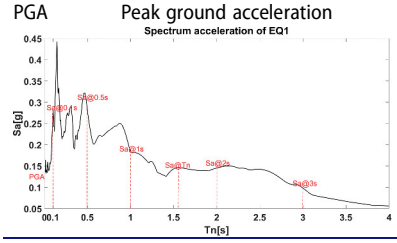

the program to ensure ANN robustness over a wide range of potential modeling cases for MT rocking walls. For specific design cases, more detailed calculation of damping ratio of mass timber rocking wall system can be found in other research (Isopescu and Gavriloaia 2015; Magalhaes, Brincker, and Cunha 2007; Mugabo, Barbosa, and Riggio 2019). In summary, the input/output configuration of the proposed ANN is designed to create a direct connection between ground motion input, lateral system design parameters, and dynamic displacement results. Similarly, instead of using the entire time history of a ground motion record as input, only a few points on the response spectrum curve were used. It will be demonstrated later that such a simple representation of the earthquake record will be able to provide enough information for reasonable maximum drift approximation.

With the input and output layers defined, the rest of the ANN is setup with 2 hidden layers with a dropout function (Serivastava et al. 2014) with a 10% drop rate, as is shown in Fig. 2. The number of nodes in the hidden layers was 197 for the first layer and 196 for the second. These specific node numbers were first selected based on experience and later optimized during training by applying Genetic Algorithm (i.e., searching for the best node number combinations to provide the best outcome). The ANN and training process were implemented using python Keras package from Tensorflow platform (François 2015).

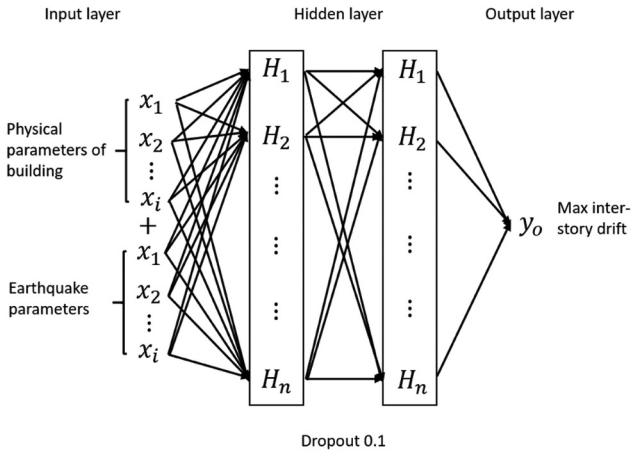

Figure 2. Example ANN architecture.

3. Training Data

The proposed ANN can be trained using dynamic response data (either real or simulated) of multi-story mass timber building with the rocking wall lateral system. Since realistic response data for this innovative system is currently not available, simulated data from time history integration was used in this study. An earlier study (Pei et al. 2021) developed and validated a simplified numerical model for PT mass timber rocking walls for balloon-framed building structures. In this model, building diaphragms and the distributed seismic mass is modeled as lumped mass at each story, the rocking walls are modeled as linear beam elements with a non-linear rotational spring at the base (see Fig. 3a). The parameters for the non-linear rotational spring are calculated based on the location and size of the PT and energy dissipation elements. The performance of non-linear hysteresis of the rotational spring for a typical mass timber rocking wall is shown in Fig. 3b. The detailed derivation of this numerical model can be found in Pei et al. (2021). For any PT rocking wall structure that can be represented by the ANN parameters outlined in Table 1, a corresponding numerical model can also be built using this simplified approach.

In order to make the proposed ANN framework general, training data was generated by randomly drawing building designs from the following realistic ranges for design parameters shown in Table 2.

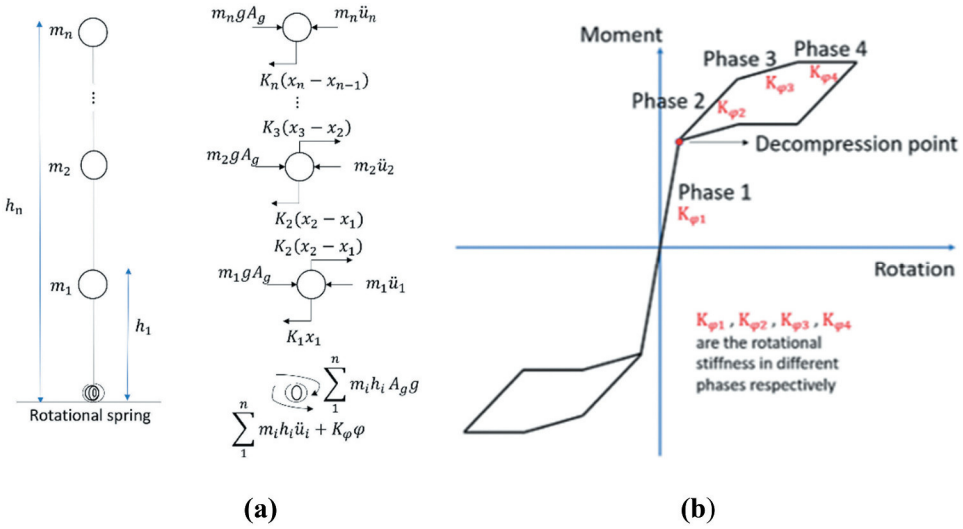

Figure 3. (a) Dynamic equilibrium of the system. (b) Non-linear hysteresis of rotational spring.

Table 2. Input parameter ranges.

Parameters	Range	Comments
N_{st}	1–18	The max story number of wood buildings is 18 by IBC
m_1	8.75 t-350.17 t	Total tributary floor mass to each rocking wall
h_1	2.44 m-7.62 m	Story height
ζ	0.01–0.20	Typical damping ratio for mass timber buildings
E_{clt}	6.89Gpa-24.82Gpa	Elastic modulus of CLT rocking wall panel
AR	1–10	Aspect ratio of rocking wall panel
t	7.62 cm-63.5 cm	Typical thickness of 3-ply to double 11-ply CLT panel
F_{ini}/F_y	0.05–0.9	Post tension ratio
A_{pt}	32.3cm^2–322.6cm^2	Total area of PT cross-section
$K0_{ufp}$	1.2kN/mm-383.2kN/mm	Total initial stiffness of UFP device
dy_{ufp}	0–254 mm	Yielding deformation of UFP device

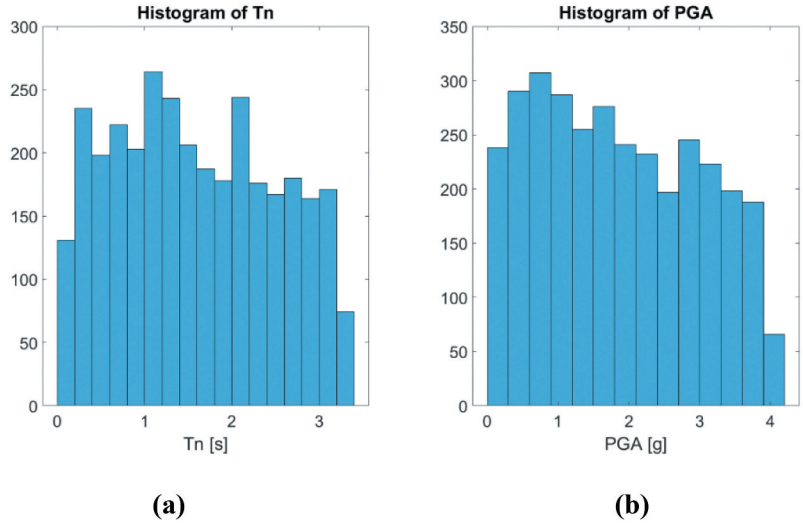

Figure 4. Histogram of training dataset (a) Fundamental period Tn of the building designs, (b) PGA of the ground motions used.

Since it is well known that seismic response of any building structure is closely related to the natural period of the building, the natural period of the building design samples was filtered in order to achieve an approximately uniform distribution between 0 and 3 s, representing the most realistic building designs. Eventually, a total of 3243 building designs were included in the training database, with the distribution of Tn is shown in Fig. 4a. This is well-representative of the possible height of mass timber buildings, as it is very unlikely the natural period of an 18-story building (IBC height limit for mass timber buildings) will be longer than 3 s.

The ground motion suite used to generate training dataset was adopted from the CUREE Woodframe project (Fischer et al. 2001). A total of 20 earthquake ground motions were divided into training and validation datasets as it is shown in Table 3. These ground motions were scaled to different intensity levels. With different scaling factors applied to the training GMs, a total of 30

Table 3. Information of ground motions.

	EQ	Year	Record ID	Earthquake event	Station	PGA(g)
Training	1	1992	CM92for	Cape Mendocino	Fortuna	0.116
	2	1992	CM92rio	Cape Mendocino	Rio Dell Overpass	0.385
	3	1992	LD92dsp	Landers	Desert Hot Springs	0.529
	4	1992	LD92yer	Landers	Yermo Fire Station	0.152
	5	1989	LP89cap	Loma Prieta	Capitola	0.529
	6	1989	LP89g03	Loma Prieta	Gilroy Array #3	0.555
	7	1989	LP89g04	Loma Prieta	Gilroy Array #4	0.417
	8	1989	LP89gmr	Loma Prieta	Gilroy Array #7	0.226
	9	1989	LP89hda	Loma Prieta	Hollister Diff. Array	0.279
	10	1989	LP89wvc	Loma Prieta	Saratoga – W Valley Coll.	0.332
Validation	11	1994	NR94mul	Northridge	Beverly Hills 14145 mulhol	0.416
	12	1994	NR94cnp	Northridge	Canoga Park – Topanga Can	0.356
	13	1994	NR94glp	Northridge	Glendale – Las Palmas	0.357
	14	1994	NR94hol	Northridge	LA – Hollywood Stor FF	0.231
	15	1994	NR94far	Northridge	LA – N Faring Rd	0.273
	16	1994	NR94cec	Northridge	N. Hollywoord – Coldwater Can	0.271
	17	1994	NR94gle	Northridge	Sunland – Mt Gleason Ave.	0.157
	18	1987	SH87bra	Superstition Hills	Brawley	0.116
	19	1987	SH87icc	Superstition Hills	El Centro Imp. Co. Cent.	0.258
	20	1987	SH87pls	Superstition Hills	Plaster City	0.186

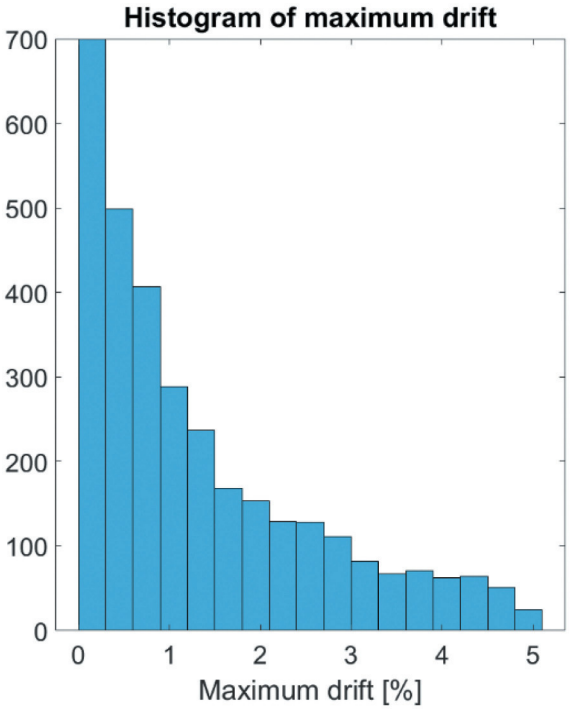

Figure 5. Histogram of training data maximum drift.

ground motions were generated with the distribution PGA shown in Fig. 4b. It can be seen that training data PGA ranges from 0 to 4 g, which covers most of the realistic hazard levels considered in design. After conducting nonlinear time history simulation of the design samples under the scaled ground motion suite, the maximum drifts from these analyses were extracted (histogram is shown in Fig. 5). By pairing the input design and ground motion parameters with maximum drift output, a training dataset for the proposed ANN was obtained. Note that the validation GMs were not used or referenced in the training process. Those GMs will later be used as validation for the accuracy of the trained ANN.

4. ANN Validation

Initially, this study aimed at training a single ANN model that can predict all design cases with reasonable confidence. However, it was discovered that a single model across all the natural period range will very likely become over-fit and biased towards certain Tn range. Thus, adjustment was made to split the training into two ANN models that predict short period and long period systems separately (the models were split at Tn = 2s). While more natural period segments may be more accurate, this study adopted a two-segment model for the balance of accuracy and complexity. From an implementation standpoint, once trained, these two models can be combined into a single algorithm with a Tn assessment at the beginning, with very little impact on overall computational efficiency.

Figure 6a shows the ANN prediction and the numerical simulated targets used for the training validation process (using only training data set), the training RMSE (root mean square error) is 0.1552. a total of 350 epochs used to improve the model accuracy, Fig. 6b shows the model loss function values during the 350 epochs. The loss function of the ANN is MSE (mean square error).

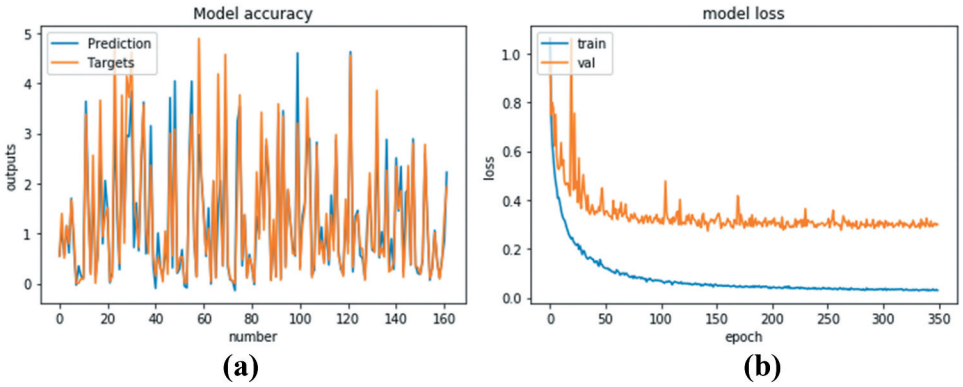

Figure 6. (a) Training performance, (b) Model loss during training.

Once the training of the ANN model was complete, five example rocking wall designs (shown in Table 4) were used to evaluate ANN maximum drift outputs in a typical setting of a displacement-based design analysis scenario. In Table 4, the demonstration of the five example buildings is listed in 3 parts. The first part is the basic building parameters and rocking wall configuration, such as story number (N_{st}), story mass (m), story height (h), CLT rocking wall panel elastic modulus (E_{CLT}), aspect ratio of rocking wall panel (AR), thickness of the rocking wall panel (t_{wall}), natural period of the building (T_n), spectrum acceleration (S_a) and damping ratio (ξ). The second part is the information of the post-tension bars, such as PT bar numbers (N_{PT}), total cross area of PT bars (A_{PT}), post tension ratio (F_{ini}/F_y), initial post tension force (F_{ini}) and yielding stress of PT bars (f_y). The last part is the parameters of the UFP devices, such as number of UFP (N_{ufp}), initial stiffness of UFP (K_{UFP}), width of the UFP plate (b_u), thickness of the UFP plate (t_u), radius of the UFP plate (D_u), yielding force of the UFP (Fy_{ufp}), yielding

Table 4. Information of example buildings.

Building information									
Ex	N_{st}	m [t]	h [m]	E_{CLT} [kN/mm]	AR	t_{wall} [cm]	T_n [s]	S_a [g]	ζ
1	3	157.58	3.35	455.33	4	13.5	1.05	0.46	0.04
2	6	97.54	3.66	315.23	3	31.5	0.47	1.02	0.05
3	9	192.60	3.96	420.30	5	31.5	1.47	0.33	0.02
4	12	262.63	3.05	630.46	6	24.4	2.34	0.21	0.06
5	15	175.09	4.27	210.15	7	63.0	2.83	0.17	0.08
PT information									
	N_{PT}	A_{PT} [cm^2]		F_{ini}/F_y		F_{ini} [kN]		f_y [Mpa]	
1	4	11.4		0.4		329.17		723.95	
2	8	20.3		0.3		440.37		723.95	
3	6	7.9		0.5		289.13		723.95	
4	8	7.9		0.4		229.80		723.95	
5	8	20.3		0.3		440.37		723.95	
UFP information									
	N_{ufp}	K_{UFP}[kN/mm]	b_u [mm]	t_u [mm]	D_u [mm]	Fy_{ufp} [kN]	Δy_{ufp} [mm]	f_y [Mpa]	
1	6	4.77	114	10	92	40.75	9	723.95	
2	12	5.52	102	19	95	140.12	5	723.95	
3	36	2.08	114	13	159	39.70	18	723.95	
4	36	4.71	102	19	178	75.06	15	723.95	
5	30	9.35	127	25	203	145.96	15	723.95	

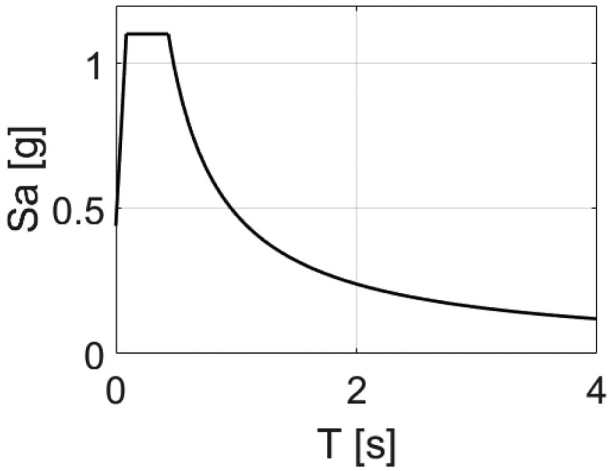

Figure 7. Design response spectrum of validation buildings.

deformation of the UFP ($\Delta y_{ufp}\Delta y_{ufp}$) and yielding stress of the UFP plate ($f_{ufp}f_y$). The 10 earthquakes in the validation set listed earlier were scaled to SLE, DBE, and MCE hazard levels were used as seismic input. The design response spectrum for the test buildings is shown in Fig. 7, representing hazard level near Seattle WA, with risk category 2 and site class C. A direct comparison between the maximum drift distribution generated by ANN and by traditional time history simulation was conducted. However, it is important to point out that the speed of ANN model is on average 18305 times faster than time-history integration (i.e., ANN model used 0.035 s to complete all analysis of the validation population (150 cases), while the traditional time history simulation took 640 s).

In context of displacement-based design, it is important to ensure the maximum drift distribution generated through ANN model will be similar to that from numerical simulation for all hazard levels of interest. In Fig. 8, these resulted drift distributions from ANN and simulation were compared for all example structures at all intensity levels. As it is shown in the figure, the simulated maximum drift data from the proposed ANN model is very similar to that from numerical integration. A T-test was also conducted for each case to compare the mean values (with p-values shown in the corresponding figure), proving the mean value of these distributions are statistically similar at 5% significance level. Considering the ability to conduct thousands of maximum displacement evaluation in a few second, the proposed ANN model could be used as a fast assessment tool for initial displacement-based design parameter selection for mass timber rocking walls.

5. Conclusions

In this study, an ANN model to compute the max drift response of mass timber buildings with post-tensioned wood rocking wall lateral system was developed. This tool was developed as an efficient alternative for time-consuming nonlinear time history analysis. The computational efficiency of the ANN model is significantly higher than time-history simulation. By comparing ANN output with a test-validated nonlinear rocking wall model, it is concluded that the model is able to achieve a reasonable level of accuracy in a PBSD context. The feasibility of the proposed ANN model here reveals a possibility of utilizing similar models for fast PBSD of CLT rocking wall system.

The ANN model proposed also has significant limitations. First of all, it was trained using one particular numerical model. The trained ANN will at best be as accurate as the model used to generate training data. It is expected that the same training process can be applied to other data

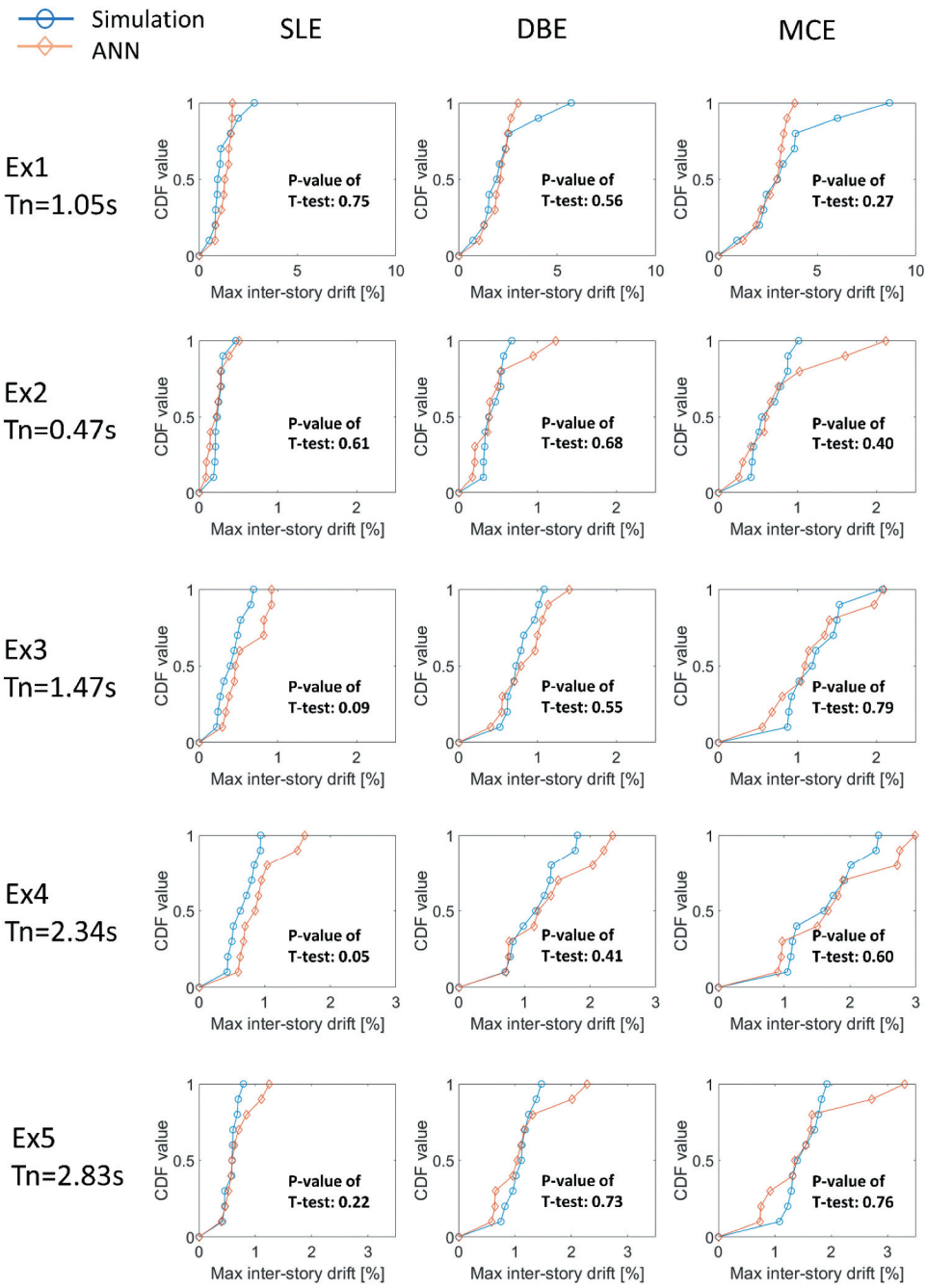

Figure 8. Comparison of maximum drift distributions.

including more advanced numerical models when they become available. Secondly, the ANN model input parameters were fixed, which means the designer can only alter these pre-defined parameters within the ranges covered by the training data set. Although the parameter ranges

adopted in this study cover most practical designs, this remains an inherent limitation for this data-driven method.

Acknowledgments

The financial support from the sponsors is greatly appreciated. The opinions and conclusions presented in this article are of the authors themselves but not the sponsors.

Disclosure Statement

No potential conflict of interest was reported by the author(s).

Funding

This research project is supported by the National Science Foundation through grant [CMMI 1636164] and U.S. Forest Services through the Wood Innovations Grant Program.

References

Abd-Elhamed, A., Y. Shaban, and S. Mahmoud. 2018. Predicting dynamic response of structures under earthquake loads using logical analysis of data. *Buildings* 8: 61. doi: 10.3390/buildings8040061.

Akbas, T., R. Sause, J. M. Ricles, R. Ganey, J. Berman, S. Loftus, J. D. Dolan, S. Pei, J. van de Lindt, and H. E. Blomgren. 2017. Analytical and experimental lateral-load response of self-centering posttensioned CLT walls. *Journal of Structural Engineering* 143 (6): 04017091. doi: 10.1061/(ASCE)ST.1943-541X.0001733.

ASCE. 2017. *Minimum design loads and associated criteria for buildings and other structures, ASCE/SEI 7–16*. Reston, VA: ASCE.

Baird, A., T. Smith, A. Palermo, and S. Pampanin. 2014. Experimental and numerical study of U-shape Flexural Plate (UFP) dissipators. NZSEE Conference, Auckland, New Zealand.

Buchanan, A., B. Deam, M. Fragiacomo, S. Pampanin, and A. Palermo. 2008. Multi-storey prestressed timber buildings in New Zealand. *Structural Engineering International* 18:2: 166–73. doi: 10.2749/101686608784218635.

Chen, Z., M. Popovski, and A. Iqbal. 2020. Structural performance of post-tensioned CLT shear walls with energy dissipators. *Journal of Structural Engineering* 146 (4): 04020035. doi: 10.1061/(ASCE)ST.1943-541X.0002569.

Fischer, D., A. Filiatrault, B. Folz, C. M. Uang, and F. Seible. 2001. Shake table tests of a two-story woodframe house. CUREE Publication No. W-06, CUREE-Caltech Woodframe Project.

François, C., others. 2015. Keras. https://keras.io .

Ganey, R., J. Berman, T. Akbas, S. Loftus, J. D. Dolan, R. Sause, J. Ricles, S. Pei, J. van de Lindt, and H. E. Blomgren. 2017. experimental investigation of self-centering cross-laminated timber walls. *Journal of Structural Engineering* 143 (10): 04017135. doi: 10.1061/(ASCE)ST.1943-541X.0001877.

Haselton, C. B., J. W. Baker, J. P. Stewart, A. S. Whittaker, N. Luco, A. Fry, R. O. Hamburger, R. B. Zimmerman, J. D. Hooper, F. A. Charney, et al. 2017a. Response history analysis for the design of new buildings in the NEHRP provisions and ASCE/SEI 7 standards: Part I – Overview and specification of ground motions. *Earthquake Spectra* 33 (2): 373–95. doi: 10.1193/032114EQS039M.

Haselton, C. B., A. Fry, R. O. Hamburger, J. W. Baker, R. B. Zimmerman, N. Luco, K. J. Elwood, J. D. Hooper, F. A. Charney, R. G. Pekelnicky, et al. 2017b. Response history analysis for the design of new buildings in the NEHRP provisions and ASCE/SEI 7 standards: Part II – Structural analysis procedures and acceptance criteria. *Earthquake Spectra* 33 (2): 397–417. doi: 10.1193/020416EQS028M.

ICC (International Code Council). 2018. *International building code*. Washington, DC: ICC.

Isopescu, D., and C. Gavriloaia. 2015. Determination of modal damping ratio for a hybrid floor system. *Journal of Vibroengineering* 17 (4): 1961–1970.

Jarrett, J. A., R. B. Zimmerman, F. A. Charney, and A. Jalalian. 2017. Response history analysis for the design of new buildings in the NEHRP provisions and ASCE/SEI 7 standards: Part IV - A study of assumptions. *Earthquake Spectra* 33 (2): 449–68. doi: 10.1193/042014EQS058M.

Jeng, C. H., and Y. L. Mo. 2004. Quick seismic response estimation of prestressed concrete bridges using artificial neural networks. *Journal of Computing in Civil Engineering* 18 (4): 360–72. doi: 10.1061/(ASCE)0887-3801(2004)18:4(360).

Lagaros, N. D., and M. Papadrakakis. 2012. Neural network based prediction schemes of the non-linear seismic response of 3D buildings. *Advances in Engineering Software* 44: 92–115. doi: 10.1016/j.advengsoft.2011.05.033.

Magalhaes, F., R. Brincker, and A. Cunha. 2007. Damping estimation using free decays and ambient vibration tests. *Proceedings of the 2nd International Operational Modal Analysis Conference* 2: 513–21.

Massari, M., M. Savoia, and A. B. Barbosa. 2017. *Experimental and numerical study of two-story post-tensioned seismic resisting CLT wall with external hysteretic energy dissipaters*. Pistoia, Italy: ANIDIS.

Moroder, D., T. Smith, A. Dunbar, S. Pampanin, and A. Buchanan. 2018. Seismic testing of post-tensioned pres-lam core walls using cross laminated timber. *Engineering Structures* 167: 639–54. doi: 10.1016/j.engstruct.2018.02.075.

Mugabo, I., A. R. Barbosa, and M. Riggio. 2019. Dynamic characterization and vibration analysis of a four-story mass timber building. *Frontiers in Built Environment* 4: Article 86. doi: 10.3389/fbuil.2019.00086.

Nazari, M., S. Sritharan, and S. Aaleti. 2017. Single precast concrete rocking walls as earthquake force-resisting elements. *Earthquake Engineering & Structural Dynamics* 56: 753–69. doi: 10.1002/eqe.2829.

Nguyen, H., H. Moayedi, L. K. Foong, H. A. H. Al Najjar, W. A. W. Jusoh, A. S. A. Rashid, and J. Jamali. 2020. Optimizing ANN models with PSO for predicting short building seismic response. *Engineering with Computers* 36: 823–37. doi: 10.1007/s00366-019-00733-0.

Pei, S., D. Huang, J. W. Berman, and S. K. Wichman. 2021. Simplified dynamic model for post-tensioned cross-laminated timber rocking walls. *Earthquake Engineering & Structural Dynamics* 50: 845–62. doi: 10.1002/eqe.3378.

Pei, S., J. W. van de Lindt, A. R. Barbosa, J. W. Berman, E. McDonnel, J. D. Dolan, H. E. Blomgren, R. B. Zimmerman, D. Huang, and S. Wichman. 2019. Experimental seismic response of a resilient 2-story mass-timber with post-tensioned rocking walls. *Journal of Structural Engineering* 145 (11): 04019120. doi: 10.1061/(ASCE)ST.1943-541X.0002382.

Perez, F. J., R. Sause, and S. Pessiki. 2007. Analytical and experimental lateral load behavior of unbonded posttensioned precast concrete walls. *Journal of Structural Engineering* 133 (11): 1531–40. doi: 10.1061/(ASCE)0733-9445(2007)133:11(1531).

Perez-Ramirez, C. A., J. P. Amezquita-Sanchez, M. Valtierra-Rodriguez, H. Adeli, A. Dominguez-Gonzalez, and R. J. Romero-Troncoso. 2019. Recurrent neural network model with Bayesian training and mutual information for response prediction of large buildings. *Engineering Structures* 178b: 603–15. doi: 10.1016/j.engstruct.2018.10.065.

Priestly, M. J. N. 1991. An overview of PRESSS research program. *PCI Journal* 36 (4): 50–57. doi: 10.15554/pcij.07011991.50.57.

Sahoo, D. M., and S. Chakraverty. January, 2018. Functional link neural network learning for response prediction of tall shear buildings with respect to earthquake data. *IEEE Transactions on Systems, Man, and Cybernetics* 48 (1): 1–10.

Serivastava, N., G. Hinton, A. Krizhevsky, I. Sutskever, and R. Salakhutdinov. 2014. Dropout: A simple way to prevent neural networks from overfitting. *Journal of Machine Learning Research* 15: 1929–58.

Wang, Y., H. Li, C. Wang, and R. Zhao. 2009. Artificial neural network prediction for seismic response of bridge structures. 2009 International Conference on Artificial Intelligence and Computational Intelligence, Shanghai, China.

Zhang, R., Z. Chen, S. Chen, J. Zhen, O. Buyukozturk, and H. Sun. 2019. Deep long short-term memory networks for nonlinear structural seismic response prediction. *Computers & Structures* 220: 55–68. doi: 10.1016/j.compstruc.2019.05.006.

Zhang, R., Y. Liu, and H. Sun. 2020. Physics-informed multi-LSTM networks for metamodeling of nonlinear structures. *Computer Methods in Applied Mechanics and Engineering* 369: 113226. doi: 10.1016/j.cma.2020.113226.

Zimmerman, R. B., J. W. Baker, J. D. Hooper, S. Bono, C. B. Haselton, A. Engel, R. O. Hamburger, A. Celikbas, and A. Jalalian. 2017. Response history analysis for the design of new buildings in the NEHRP provisions and ASCE/SEI 7 standards: Part III – Example applications illustrating the recommended methodology. *Earthquake Spectra* 33 (2): 419–47. doi: 10.1193/061814EQS087M.